International Journal of Thermophysics, Vol. 22, No. 4, 2001

Dielectric Behavior of Diamond Films[1]

H. Ye[2, 3] and P. Hing[2, 3]

Nanostructured diamond films have been synthesized using microwave plasma enhanced chemical-vapor-deposition methods. The dielectric behavior has been investigated by using impedance spectroscopy up to 500°C. Impedance data are presented in the form of a Cole–Cole plot. It is found that: (i) The resistivity contributed from both the grain interior and the grain boundary decreases with an increase of temperature. (ii) Above 250°C, the impurities at grain boundaries are thermally activated, and thus contribute to the dielectric relaxation. (iii) The electrical conductivity of diamond films follows an Arrhenius law with an activation energy transition from 0.13 and 0.67 eV at 250°C. A similar activation energy is found for the Arrhenius plot of relaxation frequencies from 0.14 to 0.73 eV. Possible physical mechanisms responsible for the dielectric behavior are presented and discussed.

KEY WORDS: diamond; dielectric; chemical-vapor-deposition.

1. INTRODUCTION

Diamond films synthesized by microwave plasma enhanced chemical-vapour-deposition methods have physical properties resembling single crystal natural diamonds including high thermal conductivity, hardness, electrical resistivity, low coefficient of friction, and high transmissivity for electromagnetic radiation [1, 2]. Recent attention has been paid to the application of diamond films to different devices such as high-temperature semiconductor devices and electronic packaging materials. The potential application of diamond in electrical and electronic devices has motivated

[1] Paper presented at the Fourteenth Symposium on Thermophysical Properties, June 25–30, 2000, Boulder, Colorado, U.S.A.

[2] Advanced Materials Research Center, School of Materials Engineering, Nanyang Technological University, Singapore 639798.

[3] To whom correspondence should be addressed. E-mail: haitaoye@yahoo.com; asphing@ntu.edu.sg

0195-928X/01/0700-1285$19.50/0

studies on the dielectric behavior over the past decades [3–7]. Most of the dielectric characterization of diamond films has concentrated on capacitance-voltage and current-voltage. Little work has been reported on the dielectric behavior of diamond films at elevated temperatures and under alternating fields, especially for the nanostructured diamond. Nanostructured diamond films are likely to have special optical, magnetic, and electronic properties [8–10]. It is, therefore, useful to characterize the dielectric properties of nanostructured diamond. In this paper, we report some interesting results on the dielectric behavior of nanostructured diamond films by using impedance spectroscopy.

Impedance measurement is a powerful tool for the study of the electric and dielectric behavior of ionic, electronic, or mixed conductor ceramics. It has been already applied successfully in the investigation of bulk properties and grain boundary properties for ferroelectric materials [11–13]. To our knowledge, the dielectric response of impedance analyzer for nanostructured diamond films has not been systematically studied.

2. EXPERIMENTAL PROCEDURES

The nanostructured diamond films were deposited on silicon substrates using a microwave plasma enhanced CVD reactor. This was reported in a previous study [14]. Commercial silicon wafer (p-type with a resistivity less than 0.05 Ω m) was chosen as the substrate. Before deposition, silicon substrates were mechanically roughened with 1 μm diamond paste in order to increase the nuclei density and then cleaned with acetone and deionized water in an ultrasonic cleaner for half an hour. It has been shown that the transition from microcrystalline to nanocrystalline diamond films can be controlled by the addition of different amounts of argon gas into the methane and hydrogen reactors [15, 16]. Therefore, during the CVD process, the $Ar/CH_4/H_2$ gas ratio, plasma power, and gas total pressure were maintained at 100/4/96 (sccm), 1.1 kW, and 30 torr, respectively. The deposition duration is 10 h, and the film thickness obtained was about 1 μm. A scanning electron microscope (SEM, JEOL-5410) was used to characterize the nanostructured diamond, and a typical micrograph of the coating is shown in Fig. 1.

The impedance data were measured over the range from 50 Hz to 1 MHz with a Fluke PM-6303 RCL meter using the two-point probe method. A schematic diagram of the impedance measurement across the film thickness is shown in Fig. 2a. The effect of current conduction through the Si substrates on the measured resistance was estimated to be less than 0.1% over the temperature range used ($\leqslant$500°C) and thus ignored [17]. Silver paste was used for an ohmic contact to the silicon substrate and

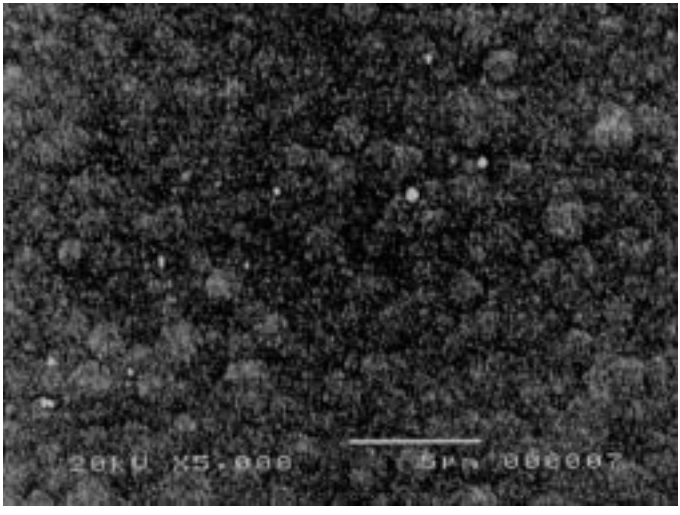

Fig. 1. SEM micrograph of the nanostructured diamond film.

diamond film, and then dried at 80°C for 1 h in order to obtain reproducible experimental data.

3. RESULTS AND DISCUSSION

The characteristic Cole–Cole plots of diamond films at different temperatures from RT to 500°C are shown in Fig. 3. It is found that each Cole–Cole plot below 250°C shows only one depressed semicircle in Fig. 3a. The single semicircle indicates that only one primary mechanism exists for the polarization within the diamond film at temperatures below 250°C [18]. The presence of the single semicircle in the frequency range

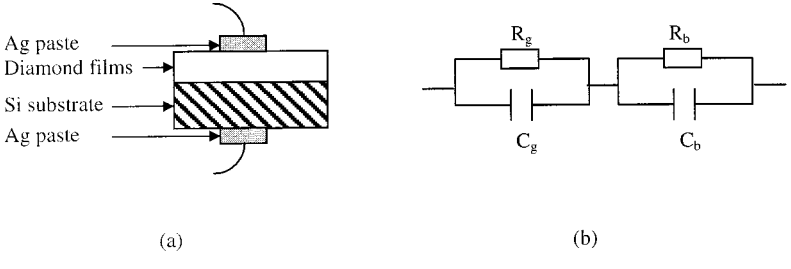

Fig. 2. (a) Schematic diagram of the impedance measurement across the film thickness and (b) circuit model for describing the dielectric property of diamond film.

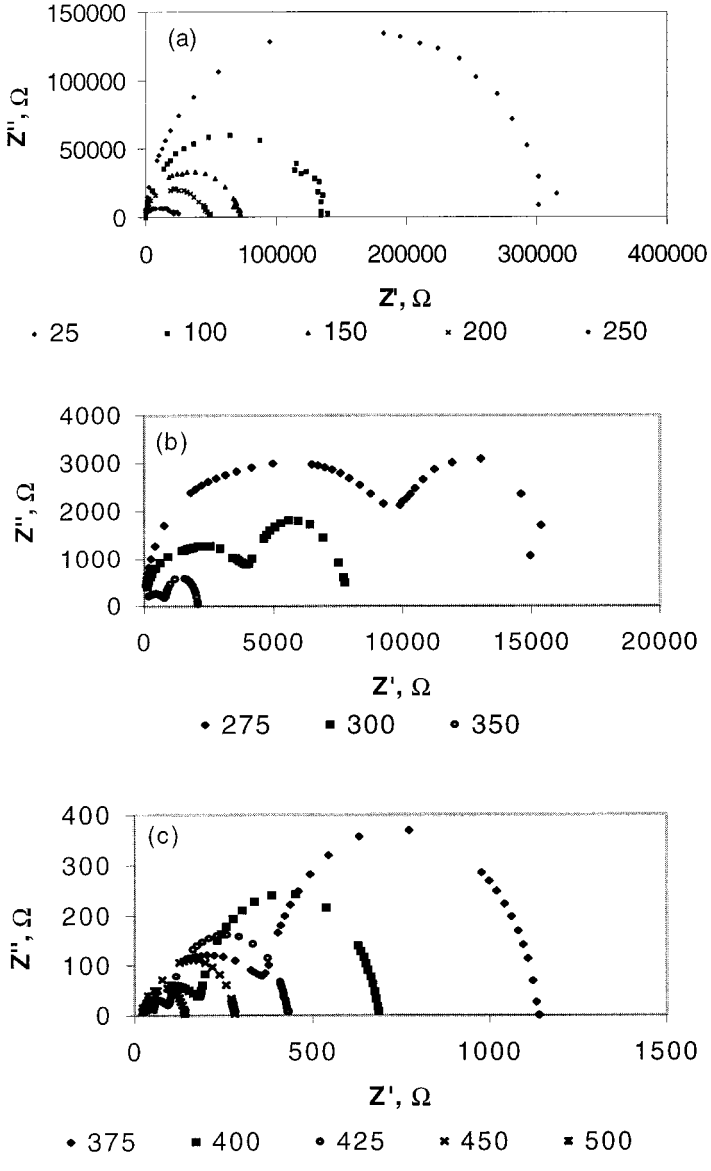

Fig. 3. Cole–Cole plots of nanostructured diamond films at different temperatures. (a) 25 to 250°C, (b) 275 to 350°C, (c) 375 to 500°C.

corresponds to the impedance response from the grain interior. The depressed semicircles make their centers on a line below the real axis, which indicates the departure from the ideal Debye behavior [19]. The second intercept of the semicircles on the real axis represents the bulk resistance of diamond films. With increasing temperature, the intercept of the semicircles shifts towards lower Z' values indicating a reduction of bulk resistance. There appears to be no secondary semicircular response in the frequency range measured and at temperatures below 250°C. Therefore, it is concluded that below 250°C, the dielectric property is dominated by the diamond grain interior.

When the temperature is raised to 500°C, the dominating dielectric relaxation mechanism changes. It is found that a secondary semicircular response occurs at elevated temperatures. In this case, two distinct semicircular relaxations were observed in Fig. 3b and c, although the high frequency response is incomplete and replaced by an arc at higher temperatures. It is possible to identify the grain interior resistance and grain boundary resistance from the visible arcs or semicircles of the Cole–Cole plots [19]. The arc on the left is assigned to the polarization within the grain interior, and the other on the right is assigned to the grain boundary. The transition of a perfect semicircle into an imperfect arc on the left or even disappearance results from a limitation of the equipment, which can only measure up to 1 MHz. The low frequency semicircular response (right) seems to become more dominant and complete with an increase of the temperature. Comparing both semicircles in each Cole–Cole plot, the relative intercept of the low frequency semicircle to the high frequency on the real axis increases with an increase in temperature, which confirms that the impedance from grain boundaries becomes more dominant at higher temperatures. In summary, Cole–Cole plots clearly demonstrate the dielectric transition from the grain interior dominating to the grain boundary dominating at about 250°C.

Usually, a double RC parallel circuit model in series [19] could be used to simulate the dielectric behavior of diamond films contributed from both grain interior and grain boundaries, as shown in Fig. 2b. Each parallel RC equivalent circuit model accurately fits each Cole–Cole semicircle. The fitting procedure used here is the same as the one described by Kleitz and Kennedy [20] and allows determination of resistance and relaxation frequencies with good precision. Here R_b and R_g correspond to the resistance contributed from the bulk grain interior and grain boundary, respectively. C_b and C_g correspond to the capacitance contributed from the bulk grain interior and grain boundary, respectively. The resistor R represents ionic or electronic conduction mechanisms, while the capacitor C represents the polarizability of the diamond. The complex impedance Z^*

measured by impedance spectroscopy can be expressed as the following function of R_b, R_g, C_b, and C_g of the specimen.

$$Z^* = Z' - jZ'' \tag{1}$$

$$Z' = \frac{R_g}{1+\omega^2 R_g^2 C_g^2} + \frac{R_b}{1+\omega^2 R_b^2 C_b^2} \tag{2}$$

$$Z'' = \frac{\omega R_g^2 C_g}{1+\omega^2 R_g^2 C_g^2} + \frac{\omega R_b^2 C_b}{1+\omega^2 R_b^2 C_b^2} \tag{3}$$

where Z' and Z'' represent the real and imaginary portions of the impedance, respectively, and ω is the angular frequency. When plotted in a complex plane, Z'' via Z' takes the form of two semicircles. In this representation, grain interior and grain boundary contributions are easily identified and the dielectric behavior of the bulk material can be studied separately from grain boundary interference.

In order to understand each semicircular relaxation process, the imaginary part of the impedance for the diamond film at different temperatures was extracted and plotted as a function of frequency. Figure 4 shows a diagram of the frequency dependence pattern of Z''. At temperatures below 250°C, only one dielectric relaxation peak was observed, as shown in Fig. 4a. It is noted that the dielectric peak shifts towards the high frequency with an increase in temperature. When the temperature increases to 250°C, two distinct dielectric relaxation peaks were observed (Fig. 4b and c). Each relaxation peak corresponds to a semicircle of the Cole–Cole plot, as shown in Fig. 3.

The relaxation frequency (f_0) of the material, independent of the geometrical parameters of the sample, is found at the apex of the Cole–Cole semicircle and is an intrinsic characteristic of the nanostructured diamond film fulfilling the condition,

$$2\pi f_0 R_b C_b = 1 \tag{4}$$

Due to the lack of impedance data on the grain boundary effect, only the electrical conductivity from the grain interior, obtained from the complex impedance plots, is plotted against inverse temperature in an Arrhenius fit (Fig. 5). The activation energy for conduction deduced from those plots was found to have a dielectric transition from 0.13 to 0.67 eV at about 250°C. Figure 6 shows the temperature dependence of the relaxation frequencies for nanostructured diamond film, which follows the same Arrhenius law from 0.14 to 0.73 eV as the electrical conductivity.

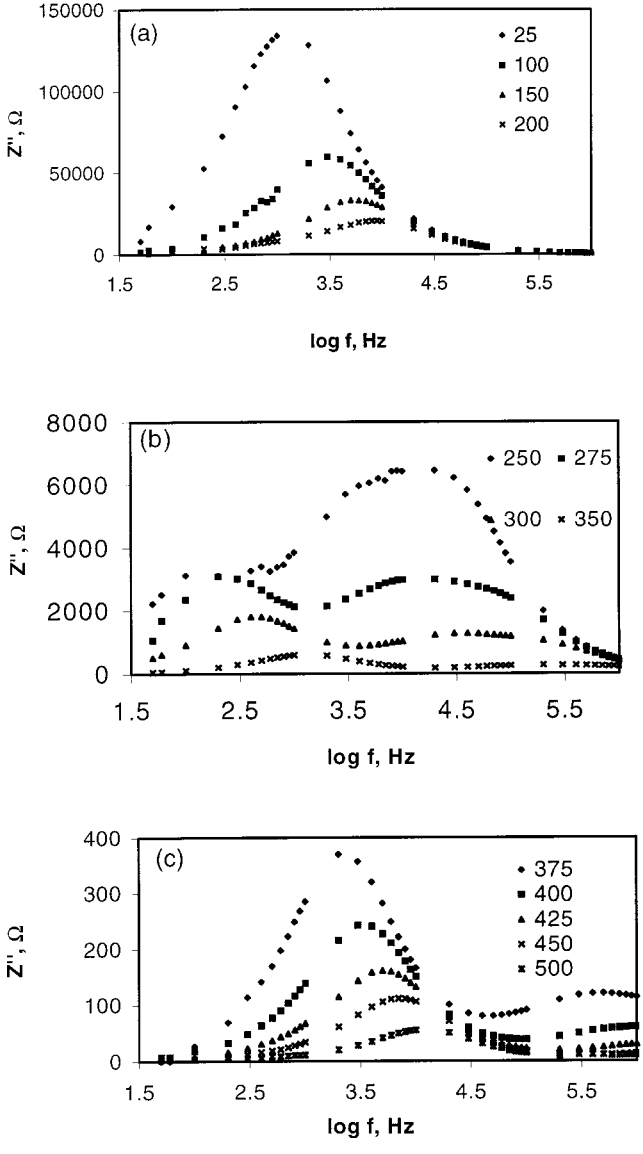

Fig. 4. Frequency dependence of imaginary part of impedance of nanostructured diamond films at different temperatures. (a) 25 to 200°C, (b) 250 to 350°C, (c) 375 to 500°C.

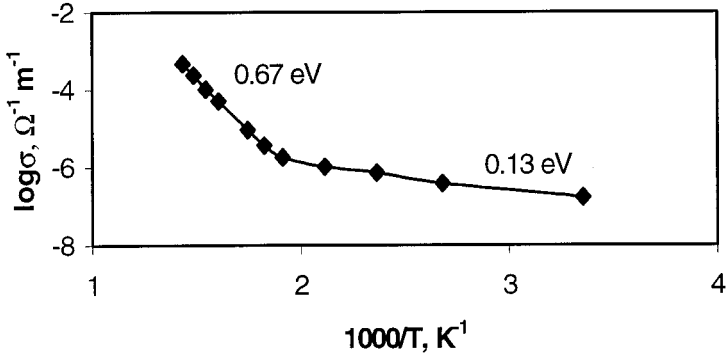

Fig. 5. Temperature dependence of grain interior electrical conductivity of nanostructured diamond films.

The physical mechanism responsible for the observed dielectric transition of nanostructured diamond film has not been completely understood, although a few researchers have reported different mechanisms to demonstrate the electrical conduction of polycrystalline diamond films. Landstrass et al. [21] proposed that the conduction transition is caused by the movements of hydrogen and defects from electrically-active deep-level sites to non-active sites during annealing. Mori et al. [22] suggested the existence of a surface conductive layer combined with chemical-absorption and oxidation. Werner et al. [23] and Huang et al. [24] have proposed space charge limited currents and the Poole–Frenkel mechanism for the nonlinear

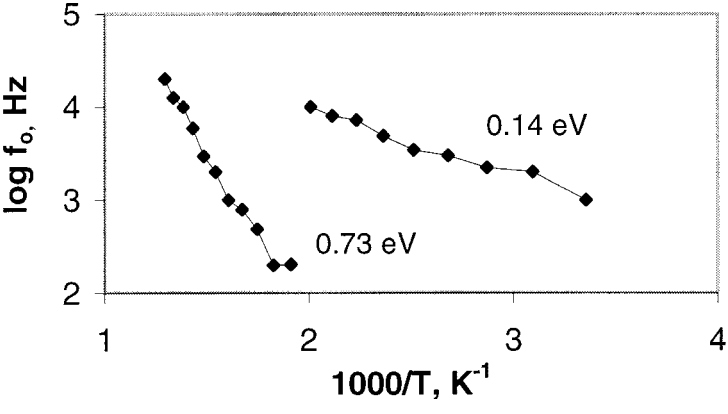

Fig. 6. Temperature dependence of relaxation frequency of nanostructured diamond films.

increase of the conduction. Frequency-independent and frequency-dependent band conduction, and the hopping conduction mechanism [25] have also been discussed in detail. More recently, a multitude of studies on the electrical conductivity of polycrystalline diamond films show that a number of defects at the grain boundaries are present that mainly influence the conduction and the mobility of the charge carriers [26, 27]. This phenomenon seems to become more obvious for nanostructured diamond films.

Nanostructured diamond films containing many fine grain boundaries, have a high surface-area-to-volume ratio [10]. The total area of grain boundaries, where defects and non-diamond carbon phases are believed to be accumulated, increases enormously [8, 9]. These impurities introduce some other electronic states in the bandgap which are normally associated with impurity level or imperfections in the lattice. These impurities are not as thermally stable as diamond grains. They are thermally activated at lower temperatures (250°C) as observed. Therefore, oxidation, diffusion, and space charge transportation can easily take place combined with an interfacial or boundary polarization arising from the accumulation and trapping of charges at the structural interface, and subsequently cause a responding secondary relaxation in impedance spectroscopy. We believe that the dielectric transition behavior originates from valence and impurity bands in the surface region of diamond films.

4. CONCLUSION

It can be concluded that the impedance data of nanostructured diamond films show the dielectric transition from the grain interior to the grain boundary dominating at about 250°C. The dielectric behavior of nanostructured diamond films can be described as a double parallel *RC* circuit in series. The bulk electrical conductivity of diamond films follows an Arrhenius law with a dielectric transition from 0.13 to 0.67 eV at 250°C. The same activation energy is found for the Arrhenius plot of relaxation frequencies from 0.14 to 0.73 eV.

ACKNOWLEDGMENT

This work is supported by the National Science and Technology Board, Singapore. One of the authors (HY) gratefully acknowledges LEE Foundation Singapore, to provide a travel award for participation of the conference.

REFERENCES

1. R. F. Davis, *Diamond Films and Coatings: Development, Properties, and Applications* (Noyes, New Jersey, 1992).
2. A. Lettington and J. W. Steeds, *Thin Film Diamond* (Chapman & Hall, London, 1994).
3. Y. Mo, Y. Xia, X. Huang, and H. Wang, *Thin Solid Films* **305**:266 (1997).
4. W. Ebert, M. Adamschik, P. Gluche, A. Flöter, and E. Kohn, *Diamond Relat. Mater.* **8**:1875 (1999).
5. S. Nath and J. I. B. Wilson, *Diamond Relat. Mater.* **5**:65 (1996).
6. Yu. V. Pleskov, Yu. E. Evstefeeva, M. D. Krotova, V. V. Elkin, A. M. Baranov, and A. P. Dement'ev, *Diamond Relat. Mater.* **8**:64 (1999).
7. A. Ibarra, M. González, R. Vila, and J. Mollá, *Diamond Relat. Mater.* **6**:856 (1997).
8. L. C. Nistor, J. Van Landuyt, V. G. Ralchenko, E. D. Obraztsova, and A. A. Smolin, *Diamond Relat. Mater.* **6**:159 (1997).
9. H. Hirai, K. Kondo, M. Kim, H. Koinuma, K. Kurashima, and Y. Bando, *Appl. Phys. Lett.* **71**:3016 (1997).
10. J. Chen, S. Z. Deng, J. Chen, Z. X. Yu, and N. S. Xu, *Appl. Phys. Lett.* **74**:3651 (1999).
11. A. Huanosta and A. R. West, *J. Appl. Phys.* **61**:5386 (1987).
12. D. C. Sinclair and A. R. West, *Phys. Rev. B* **39**:13486 (1989).
13. N. Hirose and A. R. West, *J. Am. Ceram. Soc.* **79**:1633 (1996).
14. H. Ye, C. Q. Sun, P. Hing, H. Xie, S. Zhang, and J. Wei, *Surf. Coat. Technol.* **123**:129 (2000).
15. D. Zhou, T. G. McCauley, L. C. Qin, A. R. Krauss, and D. M. Gruen, *J. Appl. Phys.* **83**:540 (1998).
16. D. Zhou, D. M. Gruen, L. C. Qin, T. G. McCauley, and A. R. Krauss, *J. Appl. Phys.* **84**:1981 (1998).
17. K. Miyata and D. L. Dreifus, *Jpn. J. Appl. Phys.* **33**:4526 (1994).
18. L. L. Hench and J. K. West, *Principles of Electronic Ceramics* (Wiley, New York, 1989), Chap. 5.
19. J. R. Macdonald, *Impedance Spectroscopy* (Wiley, New York, 1987), Chap. 4.
20. M. Kleitz and J. H. Kennedy, *Fast Ion Transport in Solids*, P. Vashishta, J. N. Mundy, and G. K. Shenoy, eds. (Elsevier, North Holland, 1979), pp. 185–188.
21. M. I. Landstrass and K. V. Ravi, *Appl. Phys. Lett.* **55**:1391 (1989).
22. Y. Mori, N. Eimori, A. Hatta, T. Ito, and A. Hiraki, *Jpn. J. Appl. Phys.* **31**:L1718 (1992).
23. M. Werner, O. Dorsch, A. Hinze, E. Obermeier, R. E. Harper, C. Johnston, P. R. Chalker, and I. M. Buckley-Golder, *Diamond Relat. Mater.* **2**:825 (1993).
24. B. Huang and D. K. Reinhard, *Appl. Phys. Lett.* **59**:1494 (1991).
25. P. Extance, S. R. Elliott, and E. A. Davis, *Phys. Rev. B.* **32**:8184 (1985).
26. D. M. Malta, J. A. von Windheim, H. A. Wynands, and B. A. Fox, *J. Appl. Phys.* **77**:1536 (1995).
27. B. Fiegl, R. Kuhnert, M. Ben-Chorin, and F. Koch, *Appl. Phys. Lett.* **65**:371 (1994).